https://doi.org/10.5194/egusphere-2026-5015
Preprint. Discussion started: 3 September 2026

Territorial deprivation and remotely mapped building damage after the 2026 Colombia earthquake: A multi-city analysis

Gelys Mestre Carrillo[1], María Isabel Castro-Rebolledo [1], Lucia C. Lozano[1]

[1]Universidad de La Salle, Bogotá, Colombia

Correspondence to: Gelys Mestre Carrillo (gmestre@unisalle.edu.co)

Abstract. Earthquake impacts reflect not only the spatial distribution of seismic shaking but also the characteristics of the territories in which exposed buildings are located. This study examined the association between territorial deprivation and remotely mapped building damage following the 10 August 2026 Colombia earthquake. We integrated Copernicus Emergency Management Service damage mapping, USGS ShakeMap ground-motion data, Overture building footprints, and census-block information from the 2018 Colombian Population and Housing Census across six urban Areas of Interest. We used a Service Deprivation Index (SDI), based on deficits in electricity, piped water, sewerage, gas, waste collection, and internet access, to characterize territorial conditions. Damage observations were spatially linked to building footprints, and grouped-binomial models assessed damage occurrence while accounting for seismic intensity and census-based covariates. Territorial deprivation varied markedly among cities and showed heterogeneous associations with mapped damage. Buenaventura exhibited a clear deprivation–damage gradient, while Pereira showed a concentration of damage in the highest deprivation quartile and a consistent positive association after adjustment. Quibdó did not reproduce this pattern. Among buildings with confirmed mapped damage, a one-standard-deviation increase in SDI was associated with approximately twice the odds of being classified as destroyed rather than damaged (OR = 2.02, 95% CI: 1.22–3.33), an association that remained consistent across sensitivity analyses. These findings indicate that seismic intensity alone does not fully characterize the spatial distribution and severity of remotely mapped earthquake damage. Integrating rapid post-event damage mapping with census-based territorial information may provide complementary evidence for identifying areas where earthquake impacts are concentrated and supporting the prioritization of post-disaster assessment and response.

1 Introduction

Earthquake impacts are not determined by the intensity of ground shaking alone. Rather, losses emerge from the interaction among seismic hazard, the exposed building stock, its physical susceptibility, and the social and material conditions of the affected population. This multidimensional perspective has progressively replaced approaches that treated vulnerability primarily as the propensity of structures to sustain physical damage. Social vulnerability encompasses the socioeconomic, demographic, institutional, and infrastructural conditions that influence the capacity of individuals and communities to anticipate, withstand, respond to, and recover from hazardous events (Cutter et al., 2003; Frigerio et al., 2019). Importantly, these conditions are spatially heterogeneous: communities exposed to comparable levels of hazard may experience substantially different consequences because their pre-existing vulnerabilities and coping capacities differ. Frigerio et al.

https://doi.org/10.5194/egusphere-2026-5015
Preprint. Discussion started: 3 September 2026

(2019), for example, emphasize that socioeconomic characteristics are inherently place-dependent and that vulnerability indicators therefore need to be interpreted within their local context rather than assumed to operate uniformly across territories.

This distinction is particularly relevant to seismic risk because social and material vulnerability interact with the characteristics of the built environment. Housing quality, construction materials, building age, height, structural system, and compliance with seismic design standards influence buildings' capacity to resist ground motion, while socioeconomic deprivation may constrain investment in safer construction, maintenance, retrofitting, and recovery. Didkovskyi et al. (2021) therefore distinguish the physical vulnerability of the building stock from the broader social and material vulnerability of the communities occupying it, while arguing that both dimensions should be considered in assessments of seismic risk. Empirical evidence from developing-country contexts reinforces this interdependence. Following the 2007 Peru earthquake, Milch et al. (2010) found that seismic intensity, construction characteristics, socioeconomic conditions, and living conditions jointly contributed to earthquake outcomes; moreover, the importance of seismic intensity decreased after accounting for building and socioeconomic characteristics in some models. Their findings also suggest that living conditions may act as a proxy for unobserved differences in investment, construction quality, and housing materials. Similarly, research on social–physical resilience after the Wenchuan earthquake emphasizes the reciprocal relationship between poverty, low educational attainment, poor-quality construction, and vulnerability of the built environment (Zhang et al., 2018).

For rapidly occurring disasters, however, detailed post-event information on structural damage is rarely available immediately and consistently over large affected areas. Remote sensing has therefore become an important component of rapid earthquake damage assessment because it provides synoptic coverage, relatively rapid acquisition, and the ability to compare large numbers of buildings across affected regions. Dong and Shan (2013) distinguish between multitemporal approaches based on pre- and post-event imagery and monotemporal approaches based exclusively on post-event observations; although the former can improve change detection, they depend on the availability of comparable pre-event data, whereas post-event approaches facilitate rapid initial assessment but can be less reliable when the pre-earthquake condition of buildings is unknown. Despite major advances in automated classification, machine learning, and deep learning, operational emergency mapping continues to rely substantially on expert visual interpretation of high-resolution imagery because of the complexity of urban scenes, limited labelled data, and difficulties in transferring automated models across events and regions (Matin and Pradhan, 2022). Recent post-earthquake reconnaissance studies further caution that remotely sensed damage products can differ from field-based assessments because of image resolution, acquisition conditions, observation geometry, classification procedures, and the limited visibility of some forms of structural damage from above (Voelker et al., 2024). Thus, satellite-based damage should be interpreted as remotely detectable building damage, rather than as a complete substitute for structural inspection.

Colombia provides a particularly relevant setting in which to examine these interactions. The country combines substantial seismic exposure with marked spatial inequalities in housing conditions, infrastructure, socioeconomic resources, and urban development. Previous Colombian studies have demonstrated the importance of integrating hazard and vulnerability information. In Pereira, Jaramillo and Campos developed seismic-loss scenarios that incorporated socioeconomic level, number of floors, roof type, building age, and use, and calibrated their models using observed damage from the 1995 and 1999 earthquakes. More recently, Feliciano et al. (2023) developed seismic-risk scenarios for residential buildings in the Sabana Centro province by integrating national census information, building exposure data, fragility and vulnerability functions, and a social vulnerability index. These studies demonstrate the value of combining physical and social dimensions of seismic risk; nevertheless, much of the Colombian literature has focused on prospective risk scenarios rather than on the spatial determinants of observed post-event damage across contrasting urban contexts. This distinction is important because modeled vulnerability

https://doi.org/10.5194/egusphere-2026-5015
Preprint. Discussion started: 3 September 2026

and realized damage do not necessarily exhibit identical spatial patterns, particularly when differences in construction practices, socioeconomic deprivation, urban morphology, and damage detectability coexist.

The Mw 7.4 earthquake that struck western Colombia on 10 August 2026 provides an unusual opportunity to examine these relationships using multiple independent geospatial data sources. The USGS ShakeMap for the event (us6000tjl2) reports a hypocentral depth of 110.3 km and provides spatially continuous estimates of Modified Mercalli Intensity (MMI), peak ground acceleration (PGA), and peak ground velocity (PGV). In parallel, the Copernicus Emergency Management Service activation EMSR916 produced rapid building-damage assessments for several affected urban areas, enabling remotely detected damage to be linked with building footprints, ground-motion estimates, and census-based indicators of territorial vulnerability. This combination makes it possible to move beyond where damage occurred and investigate whether pre-existing territorial conditions help explain its spatial distribution after accounting for differences in seismic shaking. Accordingly, this study assesses the association between territorial vulnerability and remotely sensed building damage across affected Colombian urban areas. We test three related hypotheses: (i) territorial vulnerability provides explanatory information on the occurrence of visible building damage beyond seismic ground-motion intensity; (ii) among buildings with confirmed damage, higher contextual vulnerability is associated with greater damage severity; and (iii) the magnitude and direction of the vulnerability–damage relationship vary across urban contexts rather than representing a spatially uniform effect. By integrating post-event damage mapping, ShakeMap ground-motion estimates, building-level geospatial information, and census indicators at the block level, the study aims to clarify how seismic hazard and place-based vulnerability jointly shape heterogeneous patterns of earthquake impact.

2. Materials and Methods

2.1. Study design and earthquake event

A retrospective spatial analysis examined the association between territorial conditions and building damage mapped after the 10 August 2026 Colombia earthquake. The event had a moment magnitude (Mw) of 7.4 and a hypocentral depth of 110.3 km, according to the United States Geological Survey (USGS) ShakeMap product us6000tjl2.

Following the earthquake, the Copernicus Emergency Management Service (CEMS) activated Rapid Mapping service EMSR916 to support the assessment of affected areas. Six Areas of Interest (AOIs) covered by the activation were initially considered: Northern Cali, Pereira, Cali Center, Quibdó Centre, Istmina, and Buenaventura. The analysis integrated four spatial data sources: Copernicus post-event damage mapping, USGS ShakeMap ground-motion estimates, building footprints from Overture Maps, and census information from the 2018 Colombian National Population and Housing Census (CNPV 2018).

The analytical workflow consisted of: (1) defining the portions of each AOI effectively analysed by Copernicus; (2) linking mapped damage observations to building footprints; (3) assigning seismic ground-motion estimates to the exposed buildings; (4) linking buildings to census blocks; and (5) evaluating the association between seismic shaking, census-based territorial conditions, and remotely mapped building damage.

https://doi.org/10.5194/egusphere-2026-5015
Preprint. Discussion started: 3 September 2026

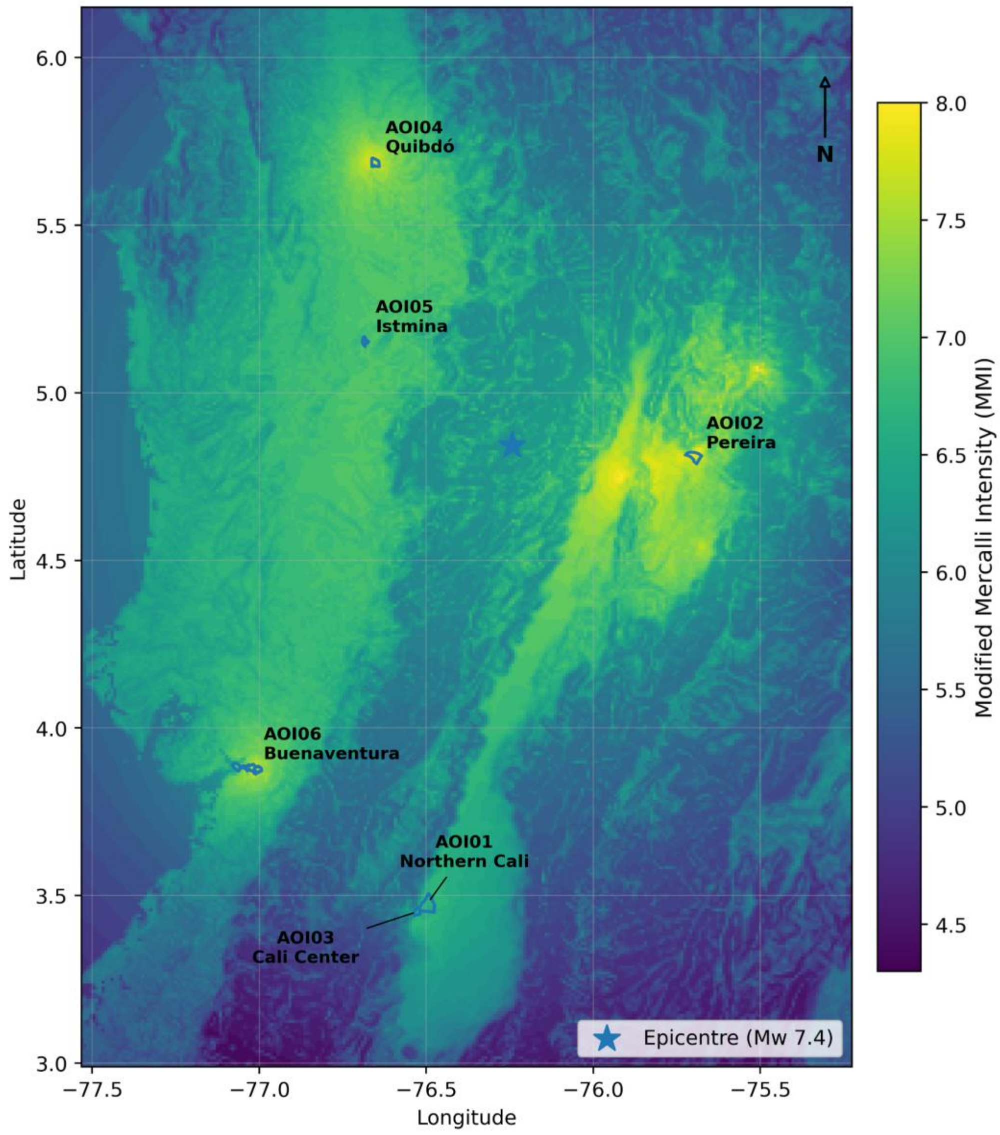

Sources: USGS ShakeMap; Copernicus Emergency Management Service (© 2026 European Union), EMSR916.

Figure 1. Location of the study areas and seismic intensity associated with the 10 August 2026 Colombia earthquake. Modified Mercalli Intensity (MMI) was obtained from the USGS ShakeMap for event us6000tjl2. The star indicates the earthquake epicentre, and the outlined polygons correspond to the six Areas of Interest (AOIs) included in the Copernicus Emergency Management Service activation EMSR916: Northern Cali, Pereira, Cali Center, Quibdó Centre, Istmina, and Buenaventura.

Sources: USGS ShakeMap; Copernicus Emergency Management Service (© 2026 European Union), EMSR916.

2.2. Copernicus post-earthquake damage data

Post-earthquake building-damage information was obtained from the grading products generated under CEMS activation EMSR916. Only portions of the AOIs effectively covered by the damage assessment were retained. Polygons identified by Copernicus as notAnalysedA were excluded before defining the building population used in the study.

The original damage layer contained 543 georeferenced observations of affected buildings, classified as Possibly damaged, Damaged, or Destroyed. These categories were retained as reported in the source product.

Copernicus damage observations were considered evidence of remotely detected damage, rather than equivalent to a field-based structural assessment. This distinction is relevant because the identification of earthquake damage from remotely sensed imagery depends on spatial resolution, viewing geometry, the characteristics of the urban fabric, the type of structural failure, and the availability of pre-event information. Reviews of post-disaster remote sensing distinguish between approaches based on pre- and post-event imagery and those relying only on post-event observations, noting that rapid post-event assessments can be constrained when the pre-disaster condition of a structure is unknown (Dong and Shan, 2013).

Despite advances in automated image classification, operational post-disaster mapping continues to involve substantial expert interpretation, particularly where heterogeneous urban environments and limited labelled training data reduce the transferability of automated approaches (Matin and Pradhan, 2022). Differences between remote-sensing assessments and field reconnaissance have also been documented in recent post-earthquake studies, particularly in relation to spatial resolution and the visibility of damage from overhead imagery (Voelker et al., 2024).

For this reason, the response variable in this study represents damage identified in the Copernicus mapping product and should not be interpreted as a complete inventory of structural damage.

2.3. Building exposure and built-environment information

Building footprints were obtained from the Overture Maps Buildings dataset. The data were extracted for the geographic extent of each AOI and subsequently clipped to the areas effectively analysed by Copernicus. Buildings intersecting areas classified as notAnalysedA were removed.

After spatial filtering, the building database contained 68,271 footprints across the six AOIs: 12,007 in Northern Cali, 17,194 in Pereira, 1,413 in Cali Center, 15,348 in Quibdó Centre, 4,826 in Istmina, and 17,483 in Buenaventura.

Building-footprint area was calculated from the polygon geometries. The num_floors attribute available in Overture was also examined as a descriptor of urban morphology. However, completeness of this variable differed substantially among AOIs. Floor-count information was sufficiently represented in Pereira and Quibdó for descriptive comparison but was sparse in several other study areas. Consequently, number of floors was not included as a common explanatory variable in the main models.

Built-environment characteristics were analysed separately from census-based territorial indicators. This distinction follows the broader seismic-vulnerability literature, in which physical vulnerability is related to attributes such as structural system, construction materials, building age, height, geometry, maintenance, and seismic design, whereas social and material vulnerability represents conditions of the population and the places in which buildings are located. Studies in Colombia have similarly incorporated building characteristics such as number of floors, age, roof type and use when modelling seismic vulnerability and expected damage.

2.4. Spatial linkage of damage observations and buildings

Copernicus damage observations and Overture buildings were provided using different geometries: affected buildings were represented by point features in the Copernicus product, whereas Overture represented buildings as polygons. A spatial matching procedure was therefore required before the datasets could be integrated.

Each Copernicus damage point was assigned to the nearest eligible Overture building, subject to a maximum distance criterion and a one-to-one matching rule. Once a building had been assigned to a damage observation, it could not be assigned to another observation.

A maximum distance of 10 m was adopted for the primary analysis. Damage observations exceeding this distance were left unmatched rather than being automatically assigned to the nearest building. Under this criterion, 430 of the 543 Copernicus observations could be linked to an Overture building.

The distance threshold was treated as an analytical decision rather than as an assumption that 10 m represents a universal positional-error limit. Therefore, the complete procedure was repeated using a 20 m threshold as a sensitivity analysis.

This conservative matching strategy was intended to reduce label-transfer errors that could arise from positional differences between independent spatial datasets, particularly in densely built areas.

2.5. Definition of the comparison building population

Buildings located within portions of the AOIs assessed by Copernicus but without a linked damage observation constituted the potential comparison population.

These buildings were not classified as structurally undamaged. Instead, they were labelled No visible damage (proxy), indicating only that no damage observation in the Copernicus product had been assigned to the building.

This distinction was maintained because remotely sensed damage inventories may fail to identify damage that is not externally visible or cannot be resolved from the imagery. Post-event-only remote-sensing approaches are particularly susceptible to this limitation when structural changes are subtle or the pre-event condition of the building is unavailable (Dong and Shan, 2013).

To reduce potential misclassification, buildings immediately surrounding unmatched Copernicus damage observations were excluded from the comparison population. These observations represented locations where Copernicus had detected damage but where the corresponding Overture footprint could not be identified with sufficient spatial confidence.

After applying these criteria, the preliminary building-level database contained approximately 67,755 buildings classified as No visible damage (proxy), 88 as Possibly damaged, 180 as Damaged, and 162 as Destroyed.

2.6. Seismic ground-motion variables

Seismic ground-motion information was obtained from the USGS ShakeMap associated with event us6000tjl2. ShakeMap provides spatial estimates of several ground-motion parameters, including Modified Mercalli Intensity (MMI), peak ground acceleration (PGA), peak ground velocity (PGV), and spectral acceleration at different periods.

MMI, PGA and PGV values were extracted from the ShakeMap grid and spatially assigned to the buildings according to their geographic location. The ShakeMap grid covering the study region had an approximate spacing of 0.009° in latitude and longitude.

https://doi.org/10.5194/egusphere-2026-5015
Preprint. Discussion started: 3 September 2026

MMI was selected as the principal ground-motion variable for multivariable modelling. PGA and PGV were retained for descriptive analyses and sensitivity assessment. This avoided simultaneously introducing highly related measures of seismic shaking into the same regression specification.

The separation between seismic hazard and vulnerability follows conventional earthquake-risk approaches in which ground motion represents the physical hazard, while the consequences of that motion depend on the characteristics of the exposed building stock and population. Previous Colombian studies have used this combination of hazard, exposure, fragility and social vulnerability to construct seismic-risk scenarios.

2.7. Census data and spatial unit of analysis

Socioeconomic and demographic information was obtained from the 2018 Colombian National Population and Housing Census (CNPV 2018) and linked to the corresponding census-block geometries from the National Geostatistical Framework.

Building centroids were spatially intersected with census blocks so that each building inherited the characteristics of the block in which it was located. Approximately 91.9% of the building footprints could be assigned to a census block, although coverage differed among AOIs.

Census information was used to characterize the territorial context surrounding the exposed buildings. It was not interpreted as information describing the socioeconomic characteristics of a particular building or its occupants.

This distinction is important when census information is used in vulnerability studies. Area-level indicators describe characteristics of places and populations aggregated within them; relationships identified at this level cannot automatically be transferred to individuals. Schmidtlein et al. explicitly identify this issue when discussing census-based social vulnerability and the potential for ecological inference.

Accordingly, census-block indicators were treated throughout the study as contextual measures of territorial vulnerability.

2.8. Census-based territorial vulnerability indicators

Variables were selected to represent dimensions of material deprivation, demographic structure, educational conditions, and household composition. Raw census counts were converted to proportions or rates when appropriate so that census blocks with different population and housing totals could be compared.

The variables considered included the proportion of dwellings without electricity, piped water, sewerage, gas, waste collection and internet access; the proportion of the population without formal education; the proportion with higher or postgraduate education; an age-dependency proxy; persons per household; and population density.

These dimensions are consistent with previous approaches to earthquake vulnerability that combine socioeconomic conditions, household characteristics, education, infrastructure, housing and characteristics of the built environment. More generally, studies of seismic vulnerability have emphasized that socioeconomic deprivation and physical characteristics of the building stock represent related but analytically distinct components of vulnerability.

Rather than combining all available variables into a general Social Vulnerability Index (SoVI), a narrower indicator was constructed to summarize deprivation in access to basic services. This decision was made because the available variables do not represent all dimensions commonly incorporated into multidimensional social-vulnerability indices and no principal-component or externally weighted SoVI procedure was applied.

https://doi.org/10.5194/egusphere-2026-5015
Preprint. Discussion started: 3 September 2026

For census block i, the Service Deprivation Index (SDI) was defined as:

$$SDI_i = \frac{p_{i,electricity} + p_{i,water} + p_{i,sewerage} + p_{i,gas} + p_{i,waste} + p_{i,internet}}{6}$$

where each term represents the proportion of dwellings in census block i **without** the corresponding service.

The index ranges theoretically from 0 to 1. A value close to 0 indicates widespread access to the six services, whereas values approaching 1 indicate increasingly widespread deprivation.

The SDI was therefore interpreted specifically as a measure of contextual service deprivation, not as a comprehensive measure of social vulnerability.

This distinction is also consistent with evidence that vulnerability indicators are sensitive to geographical context and that the same socioeconomic variables may not have identical relevance across different places. Frigerio et al. argue that vulnerability assessments need to account for local socioeconomic configurations rather than assuming that indicators have spatially uniform effects.

2.9. Descriptive analysis

Damage frequency and building exposure were first summarized for each AOI. Ground-motion variables and census-based indicators were compared among damage categories and study areas.

The distribution of the SDI was examined within each city to distinguish between absolute levels of deprivation and within-city variation. This distinction became relevant because cities with high average deprivation may nevertheless present different degrees of internal socioeconomic differentiation.

Built-environment characteristics were also summarized by AOI. Building-footprint area was available for the complete exposure dataset, whereas number of floors was reported only for buildings with valid Overture information. Because missingness in floor information differed substantially among cities, comparisons involving this variable were treated as descriptive rather than inferential.

2.10. Modelling occurrence of remotely detected building damage

The primary outcome represented the occurrence of a mapped damage observation. For the initial specification:

$$Y = \begin{cases} 1, & \text{Possibly damaged, Damaged, or Destroyed} \\ 0, & \text{No visible damage (proxy)} \end{cases}$$

An important feature of the data structure was that all buildings located within the same census block shared the same census-derived contextual variables. Treating each building as an independent observation for these variables would therefore artificially inflate the effective socioeconomic sample size.

For this reason, the main inferential analysis was conducted at census-block level. For each block, the number of buildings with mapped damage and the total number of eligible buildings were calculated. Damage occurrence was then modelled as a grouped-binomial response.

This analytical scale is consistent with the interpretation of census-based vulnerability indicators as characteristics of places rather than individual buildings.

Three nested specifications were evaluated.

The baseline model included seismic intensity and study area:

$$\mathrm{M1{:}\ Damage} \sim \mathrm{MMI} + \mathrm{AOI}$$

The second model added census-based territorial characteristics:

$$\mathrm{M2{:}\ Damage} \sim \mathrm{MMI} + \mathrm{AOI} + \mathrm{SDI} + \mathrm{Education} + \mathrm{Dependency} + \mathrm{HouseholdSize}$$

The third model allowed the association between service deprivation and damage to differ among study areas:

$$\mathrm{M3{:}\ Damage} \sim \mathrm{MMI} + \mathrm{AOI} + \mathrm{SDI} + \mathrm{Education} + \mathrm{Dependency} + \mathrm{HouseholdSize} + \mathrm{SDI} \times \mathrm{AOI}$$

Continuous predictors were standardized before model fitting. Consequently, odds ratios for continuous variables represent the change in the odds of mapped damage associated with a one-standard-deviation increase in the corresponding predictor.

Models were compared using Akaike's Information Criterion (AIC), residual deviance, odds ratios and 95% confidence intervals.

Evidence of overdispersion was observed in the grouped-binomial models. Inferential uncertainty was therefore adjusted for dispersion, and interpretation emphasized effect sizes, confidence intervals and consistency across alternative model specifications rather than relying exclusively on nominal significance levels.

2.11. Assessment of territorial heterogeneity

The association between SDI and damage was not assumed to be spatially constant. The SDI × AOI interaction was introduced specifically to test whether the relationship between contextual deprivation and mapped building damage differed among urban areas.

The principal inferential comparison was restricted to Pereira, Quibdó and Buenaventura, which contained sufficient numbers of affected buildings for city-specific estimation. Northern Cali, Cali Center and Istmina were retained in descriptive analyses but were not used to draw city-specific inferential conclusions because of the small number of mapped damaged buildings.

This approach was supported by previous work showing that socioeconomic vulnerability is place-dependent and that the relative importance of individual indicators can vary substantially among geographic contexts.

2.12. Damage severity analysis

A separate analysis was conducted to determine whether territorial conditions were associated not only with the occurrence of mapped damage but also with its severity.

Possibly damaged observations were excluded from this analysis because this category reflects uncertainty in damage identification and was not treated as an ordinal structural-damage level.

The severity analysis therefore included only buildings classified by Copernicus as Damaged or Destroyed, with the response defined as:

$$Y_{severy} = \begin{cases} 1, & \text{Destroyed} \\ 0, & \text{Damage} \end{cases}$$

https://doi.org/10.5194/egusphere-2026-5015
Preprint. Discussion started: 3 September 2026

Logistic regression was used to evaluate the association between destruction and seismic intensity, AOI and census-based territorial indicators. As in the occurrence analysis, continuous predictors were standardized to facilitate comparison of effect sizes.

This analysis was interpreted conditionally: it estimates factors associated with being classified as Destroyed among buildings already identified as having confirmed remotely detectable damage.

2.13. Sensitivity analyses

A series of sensitivity analyses was conducted to assess whether the principal findings depended on decisions made during data integration and outcome definition.

First, the Copernicus–Overture spatial linkage was repeated using maximum distances of 10 and 20 m.

Second, occurrence models were estimated both including and excluding the Possibly damaged category. In the latter specification, only Damaged and Destroyed observations were considered confirmed mapped damage.

For the occurrence sensitivity analyses, city-specific SDI effects were re-estimated under each combination of spatial-linkage threshold and damage definition. These sensitivity estimates were used to assess the stability of the direction and magnitude of the deprivation–damage association within each urban area and are therefore not numerically identical to the city-specific contrasts derived from the principal joint grouped-binomial interaction model (M3).

Third, models were repeated after excluding Quibdó to evaluate the extent to which the overall evidence of territorial heterogeneity depended on this urban context.

Fourth, the severity models were estimated under both spatial-linkage thresholds and with and without Quibdó.

The direction, magnitude and uncertainty of the estimated associations were compared across specifications. Robustness was interpreted primarily in terms of consistency of odds ratios and confidence intervals rather than whether an effect crossed an arbitrary significance threshold in every model.

All data processing, spatial integration, statistical analyses, and visualization were performed in Python using pandas, NumPy, GeoPandas, statsmodels, and Matplotlib. The complete analytical workflow and code are available in the reproducibility repository (Mestre, 2026).

3. Results

3.1. Building exposure and mapped earthquake damage

The six Areas of Interest comprised 68,271 building footprints located within areas effectively analysed by Copernicus. Building exposure varied considerably among AOIs, ranging from 1,413 buildings in Cali Center to 17,483 in Buenaventura. The Copernicus grading products contained 543 georeferenced observations of affected buildings across the study areas.

Using the primary 10-m spatial-linkage criterion, 430 Copernicus damage observations were successfully assigned to Overture building footprints. After excluding non-analysed areas and buildings located close to unmatched damage observations, the analytical building database comprised approximately 67,755 buildings classified as No visible damage (proxy), 88 as Possibly damaged, 180 as Damaged, and 162 as Destroyed.

https://doi.org/10.5194/egusphere-2026-5015
Preprint. Discussion started: 3 September 2026

The spatial distribution of mapped damage was markedly heterogeneous among AOIs. Pereira and Buenaventura accounted for most of the confirmed damaged and destroyed buildings, whereas relatively few mapped damage observations occurred in Northern Cali, Cali Center, and Istmina. Quibdó showed an intermediate number of mapped affected buildings but a damage composition that differed from that observed in Pereira and Buenaventura.

Table 1. Building exposure and remotely mapped earthquake damage across the six study areas.

Study area	Building footprints	Possibly damaged	Damaged	Destroyed	Confirmed damage
Northern Cali	12,007	1	3	1	4
Pereira	17,194	18	62	56	118
Cali Center	1,413	2	0	3	3
Quibdó Centre	15,348	47	7	15	22
Istmina	4,826	0	8	1	9
Buenaventura	17,483	20	100	86	186
Total	**68,271**	**88**	**180**	**162**	**342**

Building footprints correspond to Overture buildings located within areas effectively analysed by Copernicus. Damage categories correspond to Copernicus observations successfully linked to building footprints using the primary 10-m spatial-matching criterion. Confirmed damage includes buildings classified as Damaged or Destroyed.

3.2. Territorial vulnerability differed markedly among urban areas

Substantial differences in census-based territorial conditions were observed among the study areas. The mean Service Deprivation Index (SDI) was lowest in Northern Cali (0.055) and Pereira (0.098), intermediate in Cali Center (0.182) and Buenaventura (0.331), and highest in Quibdó (0.518) and Istmina (0.647).

The contrast was particularly pronounced for access to basic infrastructure. In Quibdó, the mean proportion of dwellings without piped water across the analysed census blocks was approximately 64.4%, while the corresponding proportion without sewerage was 71.8%. In Pereira, these proportions were approximately 0.6% and 1.5%, respectively. Buenaventura showed intermediate but heterogeneous conditions, with mean proportions of approximately 24.5% without piped water and 38.7% without sewerage.

Within-city variation also differed among AOIs. In Quibdó, the SDI ranged from approximately 0.288 at the 10th percentile to 0.701 at the 90th percentile, indicating that high average deprivation coexisted with appreciable internal variation. Buenaventura showed an even wider distribution, whereas Pereira was characterized by substantially lower absolute deprivation.

https://doi.org/10.5194/egusphere-2026-5015
Preprint. Discussion started: 3 September 2026

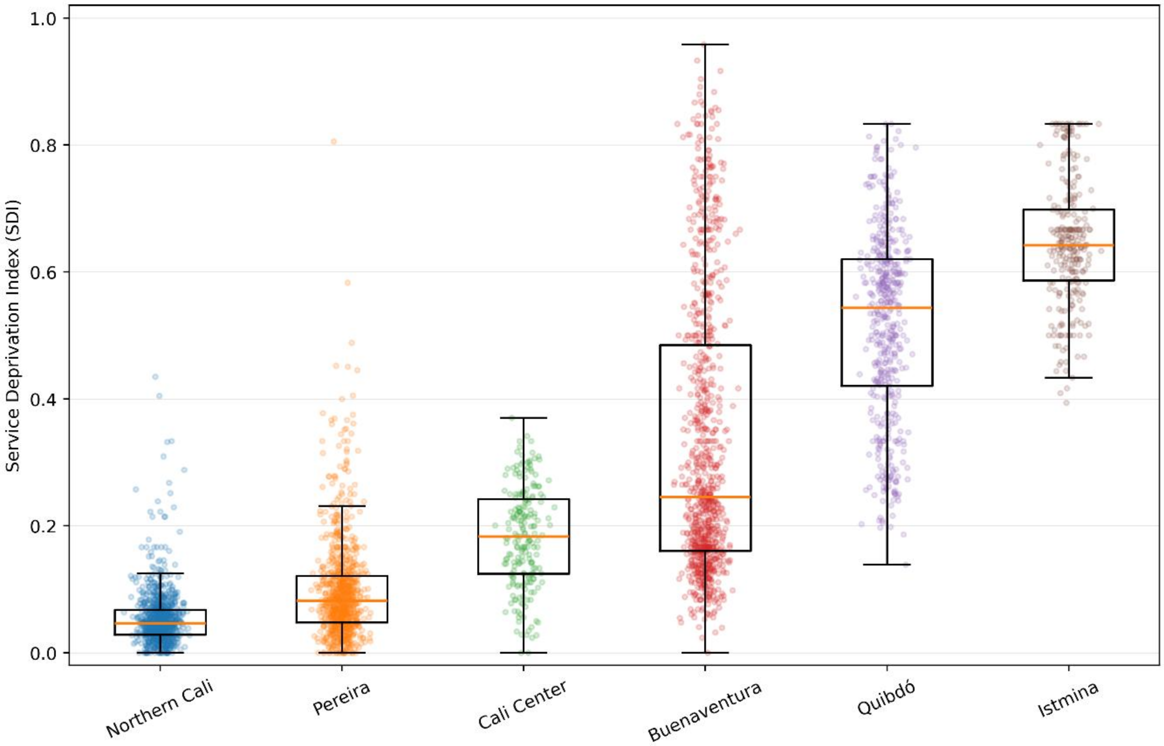

Figure 2. Distribution of the Service Deprivation Index across the six study areas. The Service Deprivation Index (SDI) was calculated at the census-block level as the mean proportion of dwellings lacking electricity, piped water, sewerage, gas, waste collection, and internet access. Higher values indicate greater deprivation in access to basic services. Boxplots represent the median and interquartile range, with whiskers extending to 1.5 times the interquartile range. Points represent individual census blocks.

3.3. Built-environment characteristics

Building morphology also differed among the study areas. Because information on number of floors was incomplete and unevenly distributed among AOIs, comparisons were restricted to cities with sufficient attribute coverage.

Floor-count information was available for approximately 58.7% of linked buildings in Quibdó and 67.4% in Pereira. Among buildings with valid floor information, 74.6% of buildings in Quibdó were one-storey structures, whereas only 3.9% had three or more floors. In Pereira, 52.1% were one-storey buildings and 13.5% had three or more floors.

Median building-footprint area was approximately 68.4 m² in Quibdó and 47.0 m² in Pereira. Because floor information was available for only a small proportion of buildings in several other AOIs, these comparisons were treated as descriptive and were not incorporated into the main inferential models.

3.4. Territorial deprivation and occurrence of mapped damage

The relationship between service deprivation and mapped building damage differed among the three principal urban areas. At census-block level, a clear monotonic increase in mapped damage was observed in Buenaventura, whereas Pereira showed a

https://doi.org/10.5194/egusphere-2026-5015
Preprint. Discussion started: 3 September 2026

marked concentration of damage in the highest deprivation quartile. Quibdó showed no comparable deprivation gradient (Figure 3).

In Buenaventura, the mapped damage rate increased progressively from approximately 0.26% among census blocks in the lowest SDI quartile to 3.33% in the highest quartile. In Pereira, damage rates decreased from 0.75% in the lowest quartile to 0.42% in the third quartile, but increased to 1.48% in the highest deprivation quartile. By contrast, Quibdó showed no monotonic pattern, with damage rates of approximately 0.56%, 0.48%, 0.26%, and 0.51% from the lowest to the highest deprivation quartile, respectively.

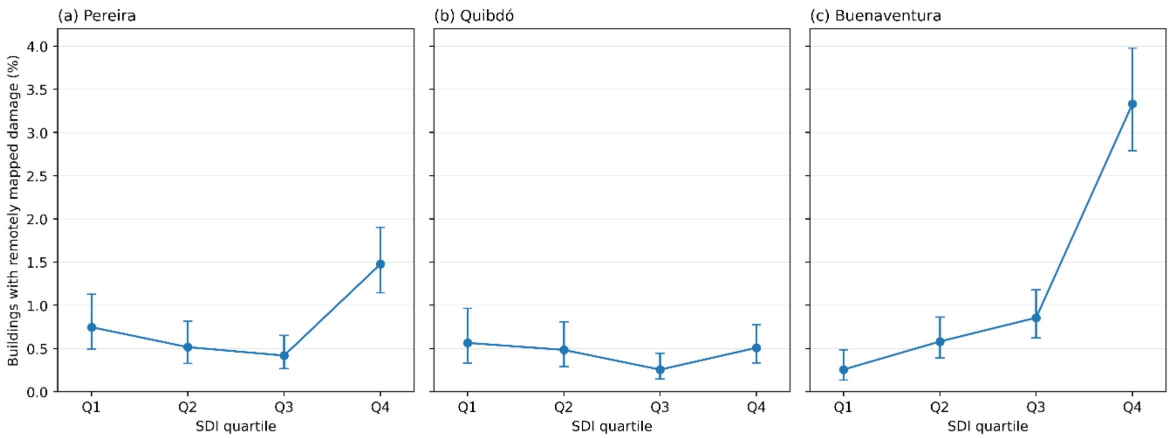

Figure 3. Remotely mapped building damage across quartiles of the Service Deprivation Index (SDI) in (a) Pereira, (b) Quibdó, and (c) Buenaventura. Bars represent the percentage of buildings associated with mapped damage within each SDI quartile. Q1 represents the lowest level of service deprivation and Q4 the highest. Buenaventura shows a progressive increase in mapped damage with increasing deprivation, whereas Pereira shows a marked concentration of damage in Q4 and Quibdó shows no monotonic deprivation–damage gradient.

3.5. Multivariable models of damage occurrence

At census-block level, models incorporating territorial vulnerability provided a substantially better fit than models containing seismic intensity and AOI alone.

The baseline model including MMI and AOI yielded an AIC of 2132.77. Adding census-based territorial variables reduced the AIC to 2051.69, whereas allowing the association between service deprivation and damage to vary among AOIs further reduced the AIC to 2000.48.

Thus:

$$\Delta AIC_{M2-M1} = -81.08$$

and:

$$\Delta AIC_{M3-M2} = -51.21$$

The interaction model therefore provided the best fit among the evaluated specifications, indicating substantial heterogeneity in the association between service deprivation and mapped damage across urban areas.

https://doi.org/10.5194/egusphere-2026-5015
Preprint. Discussion started: 3 September 2026

After adjustment for MMI and the other census-based covariates, a one-standard-deviation increase in SDI was associated with higher odds of mapped damage in Pereira:

$$OR = 1.35, \quad 95\%CI : 1.08 - 1.68$$

and a stronger association in Buenaventura:

$$OR = 2.12, \quad 95\%CI : 1.72 - 2.61$$

Quibdó showed a different pattern in this specification:

$$OR = 0.63, \quad 95\%CI : 0.44 - 0.91$$

However, the magnitude and statistical evidence for this association were sensitive to the damage definition and spatial-linkage threshold, as shown in the sensitivity analyses. Therefore, the inverse association observed in Quibdó should not be interpreted as a robust independent finding.

Persons per household showed a modest positive association with mapped damage:

$$OR = 1.20, \quad p = 0.038,$$

whereas the proportion of the population without formal education, the age-dependency proxy, and population density did not show clear independent associations in the fully adjusted specification.

Table 2. Multivariable grouped-binomial models of remotely mapped building damage in Pereira, Quibdó, and Buenaventura.

Model	Specification	Census blocks	Buildings	Damage events	AIC	Deviance
M1	MMI + AOI	2,177	43,579	354	2,132.77	—
M2	M1 + territorial vulnerability + population density	2,177	43,579	354	2,051.69	1,616.66
M3	M2 + SDI × AOI	2,177	43,579	354	**2,000.48**	**1,561.44**

Predictor	Adjusted OR	95% CI	p-value
MMI	0.65	0.56–0.75	<0.001
Persons per household	1.20	1.01–1.43	0.038
Population without formal education	1.05	0.88–1.25	0.563
Age-dependency proxy	0.86	0.70–1.04	0.119
Population density	0.98	0.82–1.16	0.791
SDI – Pereira	**1.35**	**1.08–1.68**	**0.008**
SDI – Quibdó	0.63	0.44–0.91	0.014

https://doi.org/10.5194/egusphere-2026-5015
Preprint. Discussion started: 3 September 2026

Model Specification	Census blocks	Buildings	Damage events	AIC	Deviance
SDI – Buenaventura	**2.12**	**1.72–2.61**	**<0.001**		

Note: ORs are reported for a one-standard-deviation increase in continuous predictors. SDI = Service Deprivation Index; MMI = Modified Mercalli Intensity; AOI = Area of Interest. M3 allows the association between SDI and mapped damage to vary among study areas. Inferential uncertainty was adjusted for overdispersion.

3.6. Robustness of the territorial deprivation effect

In the sensitivity analyses, city-specific SDI effects were re-estimated under alternative spatial-linkage thresholds and damage definitions. These analyses consistently reproduced the direction and general magnitude of the deprivation–damage associations observed in the principal model, although the resulting ORs are not directly equivalent to the M3 interaction contrasts reported in Table 2.

In Pereira, the adjusted odds ratio associated with a one-standard-deviation increase in SDI ranged approximately from 2.10 to 2.39 across sensitivity specifications using 10- and 20-m Copernicus–Overture linkage thresholds and including or excluding Possibly damaged.

Similarly, in Buenaventura, the corresponding estimates ranged from approximately 2.05 to 2.24.

For example:

Spatial linkage	Damage definition	Pereira OR	Buenaventura OR
10 m	All mapped damage	2.19	2.14
10 m	Confirmed damage	2.39	2.24
20 m	All mapped damage	2.10	2.05
20 m	Confirmed damage	2.29	2.13

The direction and magnitude of the associations in Pereira and Buenaventura were therefore largely insensitive to the linkage threshold or treatment of Possibly damaged.

In contrast, estimates for Quibdó were less stable and confidence intervals included or approached the null value under several sensitivity specifications. Using a 20-m linkage threshold and restricting the outcome to confirmed damage, for example, the estimated association was:

$$OR = 0.58, \quad 95\%CI : 0.29 - 1.17$$

Moreover, after excluding Quibdó, adding an interaction between SDI and city did not improve model fit, indicating that much of the detected territorial heterogeneity was associated with the distinct pattern observed in Quibdó.

https://doi.org/10.5194/egusphere-2026-5015
Preprint. Discussion started: 3 September 2026

The positive deprivation–damage gradient observed in Pereira and Buenaventura was not reproduced in Quibdó.

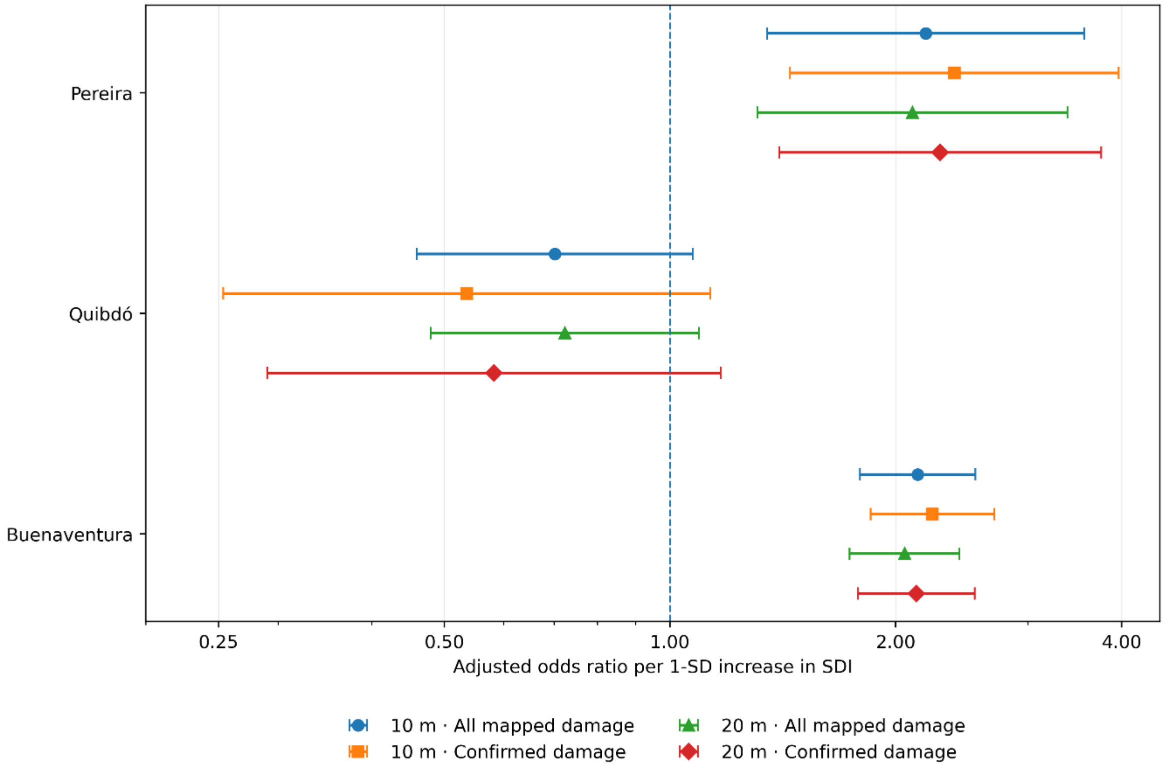

Figure 4. Robustness of the association between service deprivation and remotely mapped building damage across urban areas. Adjusted odds ratios (ORs) and 95% confidence intervals are shown for a one-standard-deviation increase in the Service Deprivation Index (SDI) under four analytical specifications combining 10- and 20-m Copernicus–Overture linkage thresholds and two damage definitions: all mapped damage (Possibly damaged, Damaged, and Destroyed) and confirmed damage (Damaged and Destroyed). The vertical dashed line indicates the null value (OR = 1).

Table 3. Multivariable analysis of damage severity among buildings with confirmed mapped damage

Model	Specification	N	Destroyed	AIC	Deviance
S1	MMI + AOI	279	133	386.673	378.673

https://doi.org/10.5194/egusphere-2026-5015
Preprint. Discussion started: 3 September 2026

S2	S1 + SDI + no formal education + age dependency + persons/household	279	133	381.767	365.767
S3	S2 + SDI × AOI	279	133	380.582	360.582

Predictor (S2)	**Beta**	**Adjusted OR**	**95% CI lower**	**95% CI upper**	**p-value**
MMI	0.423	1.527	0.907	2.573	0.111
Service Deprivation Index (SDI)	0.701	2.016	1.219	3.333	0.006
Population without formal education	-0.177	0.838	0.633	1.110	0.218
Age-dependency proxy	-0.009	0.991	0.693	1.419	0.962
Persons per household	0.058	1.060	0.703	1.595	0.782

Sensitivity specification	**N**	**Destroyed**	**Adjusted OR for SDI**	**95% CI lower**	**95% CI upper**	**p-value**
10 m; all three study areas	279	133	1.988	1.196	3.304	0.008
10 m; excluding Quibdó	262	120	1.978	1.182	3.308	0.009

https://doi.org/10.5194/egusphere-2026-5015
Preprint. Discussion started: 3 September 2026

20 m; all three study areas	304	144	1.840	1.162	2.915	0.009
20 m; excluding Quibdó	284	129	1.936	1.204	3.111	0.006

Note. The severity outcome compares Destroyed versus Damaged buildings; Possibly damaged observations were excluded. S2 is the principal severity model. ORs correspond to a one-standard-deviation increase in continuous predictors. The S3 interaction model had only a small AIC improvement and the previously evaluated global interaction was marginal; therefore, city-specific severity effects are not emphasized

3.7. Severity of confirmed building damage

A separate analysis was conducted among buildings classified as either Damaged or Destroyed. Possibly damaged observations were excluded because they did not represent a clearly ordered severity category.

Among the three principal AOIs, 279 buildings had complete information for the severity analysis, of which 133 were classified as Destroyed.

Mean seismic intensity was slightly higher among destroyed buildings than among damaged buildings. Mean MMI was approximately 7.41 for destroyed buildings and 7.36 for damaged buildings, while mean PGA was 28.76%g and 28.08%g, respectively.

After adjustment for MMI, AOI and census-based covariates, service deprivation was positively associated with destruction:

$$OR = 2.02,\quad 95\%CI : 1.22 - 3.33,\quad P = 0.006$$

Thus, among buildings with confirmed mapped damage, a one-standard-deviation increase in census-block service deprivation was associated with approximately twice the odds of being classified as Destroyed rather than Damaged.

Adding territorial vulnerability variables improved model fit relative to a specification containing MMI and AOI alone:

$$AIC: 386.67 \rightarrow 381.77$$

MMI showed a positive but statistically inconclusive association with destruction:

$$OR \approx 1.53,\ \ p = 0.111$$

No clear independent associations were observed for educational deprivation, age dependency or persons per household in the severity model.

3.8. Robustness of the severity analysis

The association between service deprivation and destruction remained consistent across sensitivity specifications.

The estimated OR ranged from approximately 1.84 to 1.99, regardless of whether a 10- or 20-m linkage threshold was applied and whether Quibdó was included.

Specifically:

$$OR_{10m} = 1.99$$

and

$$OR_{20m} = 1.84$$

After excluding Quibdó, the estimates remained similar:

$$OR_{10m} = 1.98$$

and

$$OR_{20m} = 1.94$$

All four estimates indicated a positive association between census-block service deprivation and the probability of destruction among buildings with confirmed mapped damage.

This consistency contrasted with the greater between-city heterogeneity observed for damage occurrence.

4. Discussion

4.1. Seismic intensity and territorial conditions jointly shape observed damage patterns

This study showed that the spatial distribution of remotely mapped building damage following the 10 August 2026 Colombia earthquake was not fully accounted for by differences in seismic intensity among the study areas. The inclusion of census-based territorial indicators improved model fit, and the association between service deprivation and damage varied among cities. In addition, among buildings with confirmed mapped damage, greater service deprivation was associated with higher odds of destruction. Taken together, these findings suggest that post-earthquake damage patterns need to be interpreted in relation to both the physical characteristics of the seismic event and the territorial context of the exposed built environment.

This interpretation is consistent with the conceptualization of seismic risk as the interaction among hazard, exposure, and vulnerability rather than as a direct consequence of ground shaking alone. Previous studies have shown that differences in structural systems, construction characteristics, building height, and socioeconomic conditions can produce markedly different consequences under comparable seismic exposure (Didkovskyi et al., 2021; Feliciano et al., 2023). In Colombia, seismic-risk assessments have similarly demonstrated the importance of integrating hazard information with building characteristics and socioeconomic conditions when estimating potential damage (Feliciano et al., 2023).

The improvement in model performance after incorporating census-based indicators is therefore relevant, but it should not be interpreted as evidence that lack of basic services directly increases structural fragility. The SDI used in this study represents a contextual measure of territorial deprivation, rather than a measure of building vulnerability. Census-based vulnerability indicators can capture spatial differences in access to resources, infrastructure, demographic structure, and socioeconomic conditions, but their relationship with disaster impacts depends on the characteristics of the geographical context in which they are measured (Frigerio et al., 2019; Schmidtlein et al., 2011).

This distinction is particularly important in earthquake studies because physical and social vulnerability, although related, represent different dimensions of risk. Physical vulnerability is associated with characteristics such as structural system, construction materials, building age, height, maintenance, and seismic design, whereas social and territorial vulnerability reflects the capacity of populations and places to anticipate, withstand, and recover from hazardous events (Didkovskyi et al.,

https://doi.org/10.5194/egusphere-2026-5015
Preprint. Discussion started: 3 September 2026

2021). Consequently, the association observed here between service deprivation and mapped damage may reflect territorial contexts in which socioeconomic disadvantage coexists with unmeasured characteristics of the built environment.

4.2. Territorial deprivation and damage patterns in Pereira and Buenaventura

The association between service deprivation and remotely mapped building damage was most evident in Buenaventura and, although less straightforward descriptively, was also consistently positive in Pereira. In Buenaventura, the proportion of affected buildings increased progressively across SDI quartiles, with the highest deprivation quartile concentrating substantially more mapped damage than the lower quartiles. This pattern persisted in the adjusted models and across alternative spatial-linkage thresholds and damage definitions. Pereira exhibited a different descriptive profile: damage did not increase monotonically across the entire deprivation gradient, but the highest SDI quartile showed a marked concentration of affected buildings, and the adjusted association remained positive across the sensitivity analyses.

These differences reinforce the importance of considering the spatial heterogeneity of earthquake impacts rather than assuming that socioeconomic conditions have uniform effects across territories. Pagliacci and Russo (2019) showed that the socioeconomic consequences of earthquakes can differ considerably across subregional contexts, emphasizing the relevance of spatial heterogeneity when evaluating disaster impacts. Similarly, vulnerability assessments increasingly recognize that the combination and relative importance of socioeconomic, infrastructural, and built-environment characteristics depend on local conditions (Frigerio et al., 2019; Guo and Kapucu, 2020). Thus, the differing patterns observed in Pereira and Buenaventura should not be regarded as contradictory, but rather as evidence that the relationship between territorial deprivation and earthquake damage is context dependent.

The results also support the value of analysing vulnerability at a spatial scale finer than the city as a whole. Izquierdo-Horna and Kahhat (2020) developed an interdisciplinary framework specifically aimed at identifying zones requiring priority attention after earthquakes, illustrating how spatially differentiated vulnerability information can complement conventional seismic assessments. At a territorial scale, Preciado et al. (2020) similarly demonstrated that rapid vulnerability indicators can reveal substantial spatial differences in the expected performance of masonry and adobe housing. In the present study, the census-block SDI served a comparable contextual purpose: it allowed differences within the same urban area to be examined, rather than assigning a single socioeconomic condition to an entire city.

The observed associations are also consistent with empirical evidence that socioeconomic and living conditions can modify earthquake impacts. Following the 2007 Peru earthquake, Milch et al. (2010) found that living conditions were strongly associated with injury and displacement, indicating that the consequences of seismic events are shaped by more than ground-motion intensity alone. Such findings do not imply that socioeconomic deprivation directly causes structural failure. Rather, deprivation may coexist with differences in housing quality, construction investment, infrastructure, maintenance, and other built-environment characteristics that influence how seismic shaking translates into losses.

This distinction is important for interpreting the present findings. The SDI was designed to measure deprivation in access to basic services and does not capture structural system, construction materials, building age, code compliance, or maintenance. Consequently, the positive associations observed in Pereira and Buenaventura should be interpreted as territorial associations, not as evidence that service deprivation itself increases building fragility. Physical and social vulnerability remain analytically distinct, even when they overlap spatially (Didkovskyi et al., 2021). Nevertheless, the persistence of the SDI effect across sensitivity analyses indicates that readily available census-based information can provide complementary evidence for identifying urban sectors where remotely mapped earthquake impacts are concentrated.

4.3. Quibdó as a distinct territorial context

Quibdó differed markedly from Pereira and Buenaventura in both its overall level of service deprivation and the relationship between deprivation and mapped damage. Although Quibdó exhibited substantially higher average SDI values, particularly because of deficits in piped water and sewerage, damage occurrence did not increase across deprivation quartiles. Moreover, the inverse association obtained in one model specification was not consistently reproduced in the sensitivity analyses. The evidence therefore does not support interpreting deprivation as protective; rather, it indicates that the positive deprivation–damage relationship observed in Pereira and Buenaventura was not reproduced in Quibdó.

One possible explanation concerns the context dependence of vulnerability indicators. An indicator's discriminatory capacity may decline when the underlying condition is widespread throughout the study area. Social vulnerability research has shown that both the magnitude and relative importance of individual indicators can vary substantially among geographical settings, making locally differentiated interpretations preferable to assuming spatially invariant relationships (Frigerio et al., 2019; Schmidtlein et al., 2011). In Quibdó, where service deprivation was high across much of the analysed area, SDI may therefore distinguish internal territorial differences less effectively than in a more socioeconomically heterogeneous city such as Buenaventura.

A second possible explanation concerns the built environment. Available Overture information indicated that approximately three quarters of buildings with valid floor-count information in Quibdó were one-storey structures. Building height, structural typology, construction materials, and design characteristics are known to influence seismic vulnerability and damage severity (Didkovskyi et al., 2021; Feliciano et al., 2023). However, floor information was incomplete and detailed structural characteristics were unavailable in the present dataset. The distinctive Quibdó pattern therefore cannot be attributed to its predominantly low-rise urban morphology based on the present evidence.

Remote-sensing characteristics may also have contributed to the observed pattern. Post-earthquake damage detection from satellite or aerial imagery is influenced by image resolution, viewing geometry, building density, damage type, and the visibility of structural changes from above (Dong and Shan, 2013; Matin and Pradhan, 2022; Voelker et al., 2024). Consequently, differences in mapped damage among cities may partly reflect variation in detectability in addition to differences in actual structural damage.

5. Conclusions

This study shows that the spatial distribution of remotely mapped building damage following the 10 August 2026 Colombia earthquake cannot be understood solely from differences in seismic intensity. Integrating Copernicus post-event damage mapping, USGS ShakeMap data, building footprints, and census information revealed that territorial conditions contributed additional information for explaining the observed distribution and severity of damage.

Service deprivation was associated with damage occurrence, although this relationship was not spatially uniform. Buenaventura showed a clear deprivation–damage gradient, while Pereira exhibited a concentration of damage in the most deprived areas and a consistent positive association after multivariable adjustment. Quibdó did not reproduce this pattern, highlighting the importance of considering local urban and socioeconomic contexts rather than assuming that territorial vulnerability operates similarly across cities.

A particularly relevant finding was that, among buildings with confirmed mapped damage, higher service deprivation was consistently associated with greater damage severity. Buildings located in more deprived census blocks had approximately twice the odds of being classified as destroyed rather than damaged, and this association remained stable across sensitivity analyses. This result suggests that territorial deprivation may provide useful contextual information for identifying areas where earthquake impacts are more severe, even when detailed structural inventories are unavailable.

https://doi.org/10.5194/egusphere-2026-5015
Preprint. Discussion started: 3 September 2026

These associations should not be interpreted as evidence that service deprivation directly determines structural failure. Rather, census-based deprivation may reflect broader territorial conditions that coexist with unmeasured built-environment characteristics. Identifying the mechanisms underlying the observed relationships would require detailed information on construction materials, structural systems, building age, maintenance, and seismic design.

Integrating rapid post-event remote sensing with seismic and census-based information offers a practical framework to complement conventional earthquake damage assessment. Such an approach can help identify spatial inequalities in disaster impacts and support the prioritization of field inspections and emergency response. Future applications should incorporate more detailed building inventories and field-validated damage information to determine how territorial deprivation, structural vulnerability, and seismic hazard interact in shaping earthquake losses.

Code and data availability. Post-event building damage data were obtained from the Copernicus Emergency Management Service (CEMS) activation EMSR916. Ground-motion data, including Modified Mercalli Intensity (MMI), peak ground acceleration (PGA), and peak ground velocity (PGV), were obtained from the U.S. Geological Survey (USGS) ShakeMap for event us6000tjl2. Building footprints and attributes were obtained from Overture Maps, while census-block socioeconomic information was derived from the 2018 Colombian Population and Housing Census (CNPV 2018) produced by the Departamento Administrativo Nacional de Estadística (DANE). The derived analytical dataset, spatial-matching outputs, model results, sensitivity and robustness analyses, figures, documentation, and Python code supporting this study are available from Zenodo (Mestre Carrillo, 2026).

Acknowledgements. The authors acknowledge Universidad de La Salle for the institutional support provided for the development of this research. OpenAI's ChatGPT was used during manuscript preparation to assist with language editing, code development, and manuscript organization. All analytical decisions, data processing, interpretation of results, verification of outputs, and final manuscript content were reviewed and approved by the authors, who take full responsibility for the work.

Author contributions. GMC: conceptualization, methodology, data curation, formal analysis, visualization, and writing – original draft. MICR: writing – review and editing. LCL: writing – review and editing. All authors reviewed and approved the final manuscript.

Competing interests. The authors declare that they have no conflict of interest.

Financial support. This research received no specific grant from any funding agency in the public, commercial, or not-for-profit sectors.

References

Cutter, S. L., Boruff, B. J., and Shirley, W. L.: Social Vulnerability to Environmental Hazards, Soc. Sci. Q., 84, 242–261, https://doi.org/10.1111/1540-6237.8402002, 2003.

https://doi.org/10.5194/egusphere-2026-5015
Preprint. Discussion started: 3 September 2026

Didkovskyi, O., Azzone, G., Menafoglio, A., and Secchi, P.: Social and Material Vulnerability in the Face of Seismic Hazard: An Analysis of the Italian Case, J. R. Stat. Soc. Ser. A Stat. Soc., 184, 1549–1577, https://doi.org/10.1111/rssa.12739, 2021.

Dong, L. and Shan, J.: A comprehensive review of earthquake-induced building damage detection with remote sensing techniques, ISPRS Journal of Photogrammetry and Remote Sensing, 84, 85–99, https://doi.org/10.1016/j.isprsjprs.2013.06.011, 2013.

Feliciano, D., Arroyo, O., Cabrera, T., Contreras, D., Valcárcel Torres, J. A., and Gómez Zapata, J. C.: Seismic risk scenarios for the residential buildings in the Sabana Centro province in Colombia, Natural Hazards and Earth System Sciences, 23, 1863–1890, https://doi.org/10.5194/nhess-23-1863-2023, 2023.

Frigerio, I., Zanini, F., Mattavelli, M., and De Amicis, M.: Understanding the interacting factors that influence social vulnerability: a case study of the 2016 central Italy earthquake, Disasters, 43, 867–890, https://doi.org/10.1111/disa.12403, 2019.

Guo, X. and Kapucu, N.: Assessing social vulnerability to earthquake disaster using rough analytic hierarchy process method: A case study of Hanzhong City, China, Saf. Sci., 125, 104625, https://doi.org/10.1016/j.ssci.2020.104625, 2020.

Izquierdo-Horna, L. and Kahhat, R.: An interdisciplinary approach to identify zones vulnerable to earthquakes, International Journal of Disaster Risk Reduction, 48, 101592, https://doi.org/10.1016/j.ijdrr.2020.101592, 2020.

Matin, S. S. and Pradhan, B.: Challenges and limitations of earthquake-induced building damage mapping techniques using remote sensing images-A systematic review, Geocarto Int., 37, 6186–6212, https://doi.org/10.1080/10106049.2021.1933213, 2022.

Mestre Carrillo, G.: Reproducibility dataset and code for territorial deprivation and remotely mapped building damage after the 2026 Colombia earthquake, Zenodo [data set and code], https://doi.org/10.5281/zenodo.22015938, 2026.

Milch, K., Gorokhovich, Y., and Doocy, S.: Effects of seismic intensity and socioeconomic status on injury and displacement after the 2007 Peru earthquake, Disasters, 34, 1171–1182, https://doi.org/10.1111/j.1467-7717.2010.01188.x, 2010.

Pagliacci, F. and Russo, M.: Socioeconomic effects of an earthquake: does spatial heterogeneity matter?, Reg. Stud., 53, 490–502, https://doi.org/10.1080/00343404.2018.1462483, 2019.

Preciado, A., Ramirez-Gaytan, A., Santos, J. C., and Rodriguez, O.: Seismic vulnerability assessment and reduction at a territorial scale on masonry and adobe housing by rapid vulnerability indicators: The case of Tlajomulco, Mexico, International Journal of Disaster Risk Reduction, 44, 101425, https://doi.org/10.1016/j.ijdrr.2019.101425, 2020.

Schmidtlein, M. C., Shafer, J. M., Berry, M., and Cutter, S. L.: Modeled earthquake losses and social vulnerability in Charleston, South Carolina, Applied Geography, 31, 269–281, https://doi.org/10.1016/j.apgeog.2010.06.001, 2011.

Voelker, B., Milillo, P., Tavakkoliestahbanati, A., Macchiarulo, V., Giardina, G., Recla, M., Schmitt, M., Cescon, M., Aktas, Y. D., and So, E.: The EEFIT Remote Sensing Reconnaissance Mission for the February 2023 Turkey Earthquakes, IEEE J. Sel. Top. Appl. Earth Obs. Remote Sens., 17, 19160–19173, https://doi.org/10.1109/JSTARS.2024.3476029, 2024.

https://doi.org/10.5194/egusphere-2026-5015
Preprint. Discussion started: 3 September 2026

Zhang, X., Tang, W., Huang, Y., Zhang, Q., Duffield, C. F., Li, J., and Wang, E.: Understanding the causes of vulnerabilities for enhancing social-physical resilience: lessons from the Wenchuan earthquake, Environmental Hazards, 17, 292–309, https://doi.org/10.1080/17477891.2018.1491383, 2018.